BJR

https://doi.org/10.1259/bjr.20190020

Received: 02 January 2019 | Revised: 04 March 2019 | Accepted: 07 March 2019

Cite this article as:
Ng AH, Alqahtani MS, Jambi LK, Bugby SL, Lees JE, Perkins AC. Assessing a small field of view hybrid gamma camera for perioperative iodine-125 seed localisation. *Br J Radiol* 2019; **92**: 20190020.

FULL PAPER

Assessing a small field of view hybrid gamma camera for perioperative iodine-125 seed localisation

[1,2]AIK HAO NG, PhD, [3,4]MOHAMMED S. ALQAHTANI, PhD, [3,5]LAYAL K. JAMBI, PhD, [3]SARAH L. BUGBY, PhD, [3]JOHN E. LEES, PhD and [1,6]ALAN C. PERKINS, PhD

[1]Radiological Sciences and Precision Imaging Beacon, School of Medicine, University of Nottingham, UK
[2]National Cancer Institute, Putrajaya, Malaysia
[3]Space Research Centre, Michael Atiyah Building, Department of Physics and Astronomy, University of Leicester, UK
[4]Radiological Sciences Department, College of Applied Medical Sciences, King Khalid University, Abha, Saudi Arabia
[5]Radiological Sciences Department, College of Applied Medical Sciences, King Saud University, Riyadh, Saudi Arabia
[6]Medical Physics and Clinical Engineering, Nottingham University Hospitals NHS Trust, Nottingham, UK

Address correspondence to: Dr Aik Hao Ng
E-mail: *hao06051982@yahoo.co.uk*

Objective: To examine the imaging capability of a novel small field of view hybrid gamma camera (HGC) using ^{125}I seeds prior to surgical use.

Methods: The imaging performance of the camera system was assessed quantitatively and qualitatively at different source depths, source to collimator distances (SCD), activity levels, acquisition times and source separations, utilising bespoke phantoms.

Results: The system sensitivity and spatial resolution of the HGC for ^{125}I were 0.41 cps/MBq (at SCD 48 mm) and 1.53 ± 0.23 mm (at SCD 10 mm) respectively. The camera was able to detect the ^{125}I seed at a SCD of 63 mm (with no scattering material in place) in images recorded within a 1-min acquisition time. The detection of the seeds beneath scattering material (simulating deep-seated tumours) was limited to depths of less than 20 mm beneath the skin surface with a SCD of 63 mm and seed activity of 2.43 MBq. Subjective assessments of the hybrid images acquired showed the capability of the HGC for localising the ^{125}I seeds.

Conclusion: This preliminary *ex vivo* study demonstrates that the HGC is capable of detecting ^{125}I seeds and could be a useful tool in radioactive seed localisation with the added benefit of providing hybrid optical γ images for guiding breast conserving surgery.

Advances in knowledge: The SFOV HGC could provide high resolution fused optical-gamma images of ^{125}I radioactive seeds indicating the potential use in intraoperative surgical procedure such as RSL.

INTRODUCTION

Breast cancer is the most common cancer diagnosed in females worldwide. In the United Kingdom, Cancer Research UK estimated that there were 55,122 new cases of breast cancer in 2015 and 11,563 deaths from breast cancer in 2016.[1] Due to advances in imaging technologies and national breast screening programmes, approximately 25–35% of detected breast tumours are non-palpable at diagnosis.[2,3] The accurate identification of non-palpable lesions pre- and intraoperatively, together with the precise localisation of the tumour with adequate resection margins, are crucial in the quality of surgical care and will affect the oncological and cosmetic outcomes. Wire guided localisation (WGL), where a guide wire is placed *in situ* under ultrasonographic or radiographic control, has been the standard technique for guiding the surgical resection of non-palpable breast tumours. However, this technique can cause discomfort and inconvenience to the patient.

Radioactive seed localisation (RSL) is a radioguided surgical technique to identify occult breast tumours using the insertion of an ^{125}I seed (gamma energy ~35.5 keV, having a nominal activity of between 3 and 13 MBq) at the centre of the tumour, under ultrasonographic or X-ray mammographic guidance.[4] It is an increasingly popular technique,[4,5] which was first reported by Gray et al[6] in 2001 and are now becoming standard clinical practice in a number of medical centres worldwide. A sterile gamma probe is usually used to guide the surgeon to the radioactive seed in order to locate the suspicious opacity or lesion during the surgical procedure. Compared to the conventional WGL technique, the RSL procedure has been found to be easier to perform allowing more flexibility during seed placement and for surgical incision site localisation as well as being more acceptable to the patient while having a similar oncological outcome.[7]

Figure 1. Photograph of the Oncoseed model 6711.

Pouw et al[8,9] have reported the feasibility of using Freehand Single Photon Emission CT, a unique combination of a conventional gamma probe with an optical tracking system, in RSL. The system provided continuous real time three-dimensional (3-D) gamma images with information about depth and location of the radioactive seeds, thus enabling accurate and adequate excision of the tumour. However, this system still required further optimisation in terms of spatial resolution (5 mm) and accuracy in localisation.

We propose that a small field of view (SFOV) HGC could potentially offer added value to the RSL technique due to its high spatial resolution and the ability to provide hybrid optical-gamma images. The aim of the study was to examine the imaging capability of a novel SFOV HGC with ^{125}I seeds for potential use in RSL.

METHODS AND MATERIALS

Two ^{125}I-seeds (OncoSeed™ Type 6711C, Oncura, GE Healthcare, Arlington Heights, IL) with initial activity of 8.36 and 8.33 MBq respectively were used in this study. The radioactivity of the seeds decayed over time during the experimental work, ranged between 1.4 and 8.3 MBq to cover the typical activity ranges used in RSL. The seeds measured 4.5 mm in length and were 0.8 mm in diameter as shown in Figure 1.

Imaging assessments were undertaken with two prototype versions of the HGC developed by the University of Leicester. The first camera was fitted with a 0.5 mm pinhole collimator and the modified system was fitted with a 1.0 mm pinhole collimator.[10,11] The experiments took place in the research gamma camera facility in Medical Physics, Queen's Medical Centre, Nottingham University Hospitals NHS Trust, Nottingham, UK.

Imaging capability assessments

Sensitivity and spatial resolution tests for the ^{125}I seeds using the HGC and a non-imaging gamma probe were assessed according to published references.[12,13] The system spatial resolution was measured by imaging the ^{125}I seed in place of a line source, as the diameter of the seed was smaller than the camera's resolution. These performance test results were compared to a standard large field of view (LFOV) gamma camera (Nucline™ X-Ring-R, Mediso, Hungary) within the clinical department. The gamma probe used was a Navigator GPS™ with 12 mm angled probe (RMD Instruments Corp., Watertown, MA).

Imaging performance assessments were carried out utilising bespoke phantoms[11,14] to simulate patient anatomy and tumour

Figure 2. Schematic diagram of the experimental set up using the HGC and bespoke phantoms; the HGC positioned on top of the (a) sentinel node phantom and (b) anthropomorphic breast phantom to acquire gamma images of the radioactive sources located at different configurations.

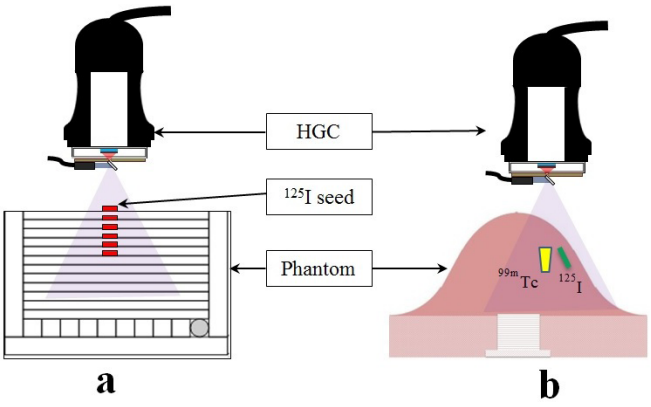

position as shown in Figure 2a. The clinical simulations explored different source depths, SCD, amounts of activity, image acquisition times and source separations. A quantitative assessment was carried out by calculating the contrast-to-noise ratio (CNR) using equation:

$$\mathrm{CNR} = \frac{N_1 - N_0}{\sigma_0}$$

where N_1 is the mean counts per pixel of the hot spot, N_0 is the mean counts per pixel in the background area and σ_0 is the standard deviation of mean counts per pixel in the background area. The detectability of the seed is related to the CNR value. This was evaluated following the Rose criterion where any hot spot with CNR value exceeding 3–5 was considered to be detectable.[15] The higher the calculated CNR, the easier it is expected to be detected visually. Quantification was carried out using ImageJ 1.47v (National Institute of Health, US). The hybrid optical-gamma images were obtained and assessed qualitatively.

Simultaneous detection of radionuclides

Considering the potential use of SFOV gamma cameras in the simultaneous detection of dual radionuclides by combining RSL and sentinel lymph node biopsy procedures,[16] a pilot experimental study was carried out using the bespoke anthropomorphic breast phantom.[11] The phantom provided cavities to hold a number of radioactive sources. An ^{125}I seed (6.25 MBq) and ^{99m}Tc solution (0.16 MBq) contained in an Eppendorf tube were inserted into the phantom. These were placed 2 cm apart (centre-to-centre) and 2 cm beneath the simulated skin surface of the phantom. Imaging was undertaken using the HGC fitted with a 1 mm pinhole collimator positioned 2 cm away from the phantom to record an axial view as shown in Figure 2b. Image acquisition time varied between 30 s and 600 s.

For comparison purposes, imaging with a conventional LFOV gamma camera (Nucline™ X-Ring-R, Mediso, Hungary) and a SPECT-CT camera system (Brightview XCT, Philips Healthcare, Milpitas, CA) was performed at the nuclear medicine clinic,

Queen's Medical Centre, Nottingham University Hospitals NHS Trust. An energy window width of 20% centred on the photopeaks of each radionuclide (30 and 140 keV respectively) was set on both camera systems for simultaneous acquisition. The SPECT-CT image registration was performed using ImageJ 1.47v (National Institute of Health, US).

Clinical simulation

Preliminary assessments were carried out to determine the ability of the SFOV gamma camera to visualise the seed in the clinical simulation. One or two ^{125}I seeds (~6 MBq each) was placed underneath the surface of the breast region of an adult cardiopulmonary resuscitation (CPR) training manikin. The surface of the manikin was marked at four pre-defined positions with the letters A to D.

Six participants (nuclear medicine professionals) were recruited to assess the ability of the HGC camera to locate the seeds. The participants were informed of the study objectives and imaging procedures and asked to locate the number and position of the located seeds based on their professional experience of nuclear medicine imaging. Imaging was undertaken using the HGC mounted with 1.0 mm pinhole collimator, positioned at SCD of 140 mm with 2 min acquisition time. The participants were asked to visually assess the resulting image to determine the position and number of seeds involved. If the first image was not satisfactory, a second image acquisition was taken with a shorter SCD focusing on the 'suspected area' as determined by the participant.

RESULTS

Imaging capability assessments

The system characteristics of the cameras for imaging ^{125}I seeds are shown in Table 1 with results for the HGC fitted with the two different sizes of collimator. The system spatial resolution of the SFOV gamma camera is higher compared to conventional LFOV gamma camera and gamma probe. In contrast, the sensitivity of the SFOV camera systems was lower than the clinical cameras mainly due to the type of pinhole collimator and thin crystal detector.

A series of gamma images with the ^{125}I seeds (2.43 MBq) at different depths between 0 and 25 mm were acquired using the HGC fitted with 1 mm diameter pinhole collimator and using an image acquisition time of 5 min. Figure 3 shows the relationship of the CNR with depth. From the acquired gamma images the CNR values ranged from 1 to 16. Similar imaging assessments

Figure 3. (Left) Relationship of CNR values and depths for the ^{125}I seed images acquired at SCD of 63 mm and acquisition time of 5 min (n = 3). (Right) Example gamma images of the seed placed at a depth of (a) 0 and (b) 20 mm underneath of Polymethyl methacrylate (PMMA) plate.

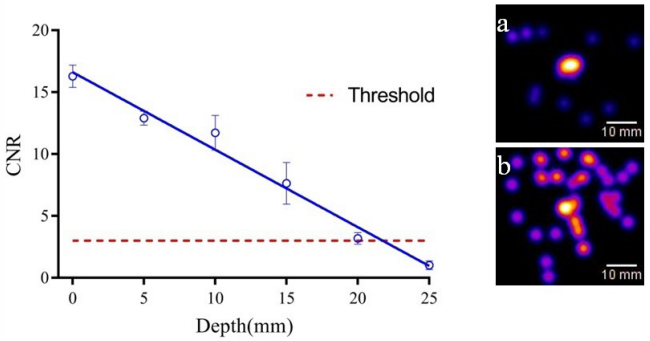

with the placement of the seed at SCD between 20 and 100 mm were also undertaken without the presence of scattering medium. The CNR values of the acquired gamma images ranged between 6 and 144 as shown in Figure 4. Both assessments have demonstrated that the relationships between CNR value and seed depths or SCDs are inversely proportional, with the deeper seed depths or further SCDs producing lower CNR values.

Images acquired over varying acquisition times at a set imaging distance (63 mm, without scattering material) were also evaluated for ^{125}I seeds with activity of 2.43 MBq. Figure 5 shows the resulting CNR values ranging between 5 and 63. In this study, the camera was able to detect the seed in all images acquired. Similarly, both CNR values increased with the increase of acquisition time.

Further imaging was carried out to investigate the ability of the HGC to differentiate two separate ^{125}I seeds (~1 MBq each). The HGC was able to resolve seeds with an edge-to-edge separation of 3 mm at a SCD of 30 mm with an acquisition time of 600 s. Figure 6 shows the gamma, optical and fused images of the two ^{125}I seeds with an edge-to-edge separation of 3 mm. With the smaller diameter pinhole collimator (0.5 mm), the camera had the capability to resolve the two ^{125}I seeds with a minimum separation of 2 mm. Figure 7 illustrates the line profiles of the acquired gamma images. Two peaks can be clearly identified in the Gaussian fitted profile generated from the gamma image acquired with the seeds placed at 2 mm apart; however, two

Table 1. Sensitivity and spatial resolution of the gamma probe, SFOV and LFOV gamma cameras

Parameter	HGC		Nucline™ TH[a]	Gamma probe
	0.5 mm pinhole	1 mm pinhole		
System spatial resolution FWHM (mm) at 10 mm	0.75 ± 0.07	1.53 ± 0.23	7.5(LEHR)	14.47 ± 0.08
Intrinsic sensitivity (cps/MBq) at 250 mm	0.25	0.22	Not available	Not available
System sensitivity (cps/MBq) at 48 mm	0.02	0.41	119 (LEGP)	233

CPS, count per second; FWHM, full width at half maximum; LEGP, low energy general purpose collimator; LEHR, low energy high resolution collimator; MBq, megabecquerel.
[a]Data taken from[17] using ^{99m}Tc source.

Figure 4. (Left) Relationship of CNR values and SCDs for the ^{125}I seed (2.43 MBq) images acquired using HGC. Image acquisition time was 5 min respectively (n = 3). (Right) Gamma images acquired at SCD of (a) 20 mm and (b) 100 mm without the presence of scattering medium.

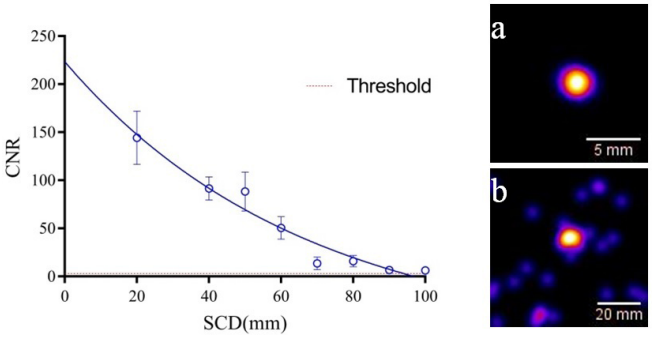

discrete peaks could not be distinguished with the seeds placed closer (1 mm apart).

Simultaneous detection of radionuclides

Figure 8 shows gamma images from the simultaneous detection of ^{99m}Tc and ^{125}I sources placed within the breast phantom using the different imaging systems. Gamma images shown on the top row (Figure 8a–c) were taken with the HGC for acquisition times of 30, 60 and 120 s. In this experiment, both radioactive sources could be detected within a 30 s acquisition time. With the increase of acquisition time, subjective visual assessment was that the demarcation of the individual sources became more distinct. Although both radionuclides could be seen, the system could not discriminate between the different gamma emission energies which may represent a limitation during clinical use. Images on the bottom row show the phantom images acquired using a LFOV gamma camera (Figure 8d) and a SPECT-CT (Figure 8e). Two hot spots can be clearly seen in both images. With the aid of the CT image, the SPECT images were fused and displayed in different colour scales (green:^{99m}Tc; hot metal: ^{125}I) to ease identification of the two different radionuclides

Figure 5. Relationship of CNR values and acquisition time for the ^{125}I seed with activity level of 2.43 MBq (n = 3). Images were acquired using HGC placed at SCD of 63 mm and acquisition time of (a) 1, (b) five and (c) 10 min. Error bars are due to higher number of noise photons.

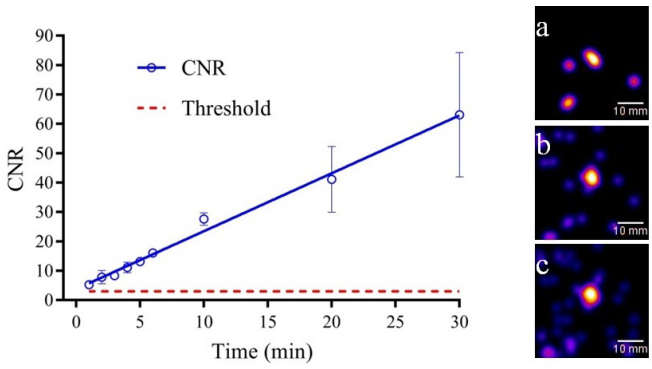

accumulated within the target tissues (simulating ^{99m}Tc source in the sentinel node and the ^{125}I seed in the primary tumour).

Clinical simulation

All six assessors were able to determine the correct number of seeds located at the designated sites by visual assessment of the hybrid images (Figure 9). Four out of the six assessors required a second image acquired at a closer SCD in order to confirm the number and location of the seeds.

DISCUSSION

Compact SFOV hybrid gamma cameras have the potential capability for improving intraoperative imaging procedures. To our knowledge, this article presents the first results of detecting and imaging the lower energy gamma photons emitted by ^{125}I seeds currently being used for RSL surgical procedures with a SFOV HGC. We consider that this technology would be particularly useful in RSL for non-palpable breast tumours and other soft tissue masses[18] and would be complementary to the current standard procedure using a gamma probe. The low sensitivity of the HGC may be a possible limitation. The intrinsic sensitivity of the Nucline™ gamma camera and the gamma probe were not available, however these are known to be significantly higher in the order of 100 s counts per second/MBq. Nevertheless we were able to obtain useful images showing the position of the seeds within acceptable imaging times.

The hybrid images may aid the surgeon in localising the seed and confirming the position with the aid of images obtained. This may also be a useful tool in assessing the clearance of radioactivity around the breast tissues and lymphatic basin following surgery and in localising the seed *ex vivo* from the excised tissue specimen. However, the usability of this imaging technology in practice must be evaluated to determine the impact on working practice and the potential for user variability.

For dual radionuclide studies, the lack of energy discrimination is a current limitation. At the time of the investigation, the camera settings allowed detection of both ^{125}I and ^{99m}Tc with the same colour image display. This limits the potential of the camera to segregate tissue masses when dual radionuclides are used simultaneously for example during combined RSL and sentinel lymph node biopsy procedures. In addition, the 2-D images do not provide any estimation of the depth of the radionuclide uptake, which would be crucial information for the more accurate excision and harvesting of the sentinel node and tumour masses.

Preliminary camera testing has revealed that SFOV hybrid gamma cameras were able to detect ^{125}I with activity levels typically used in surgery within an acceptable acquisition time. In particular, the camera was able to detect an ^{125}I seed at SCD of 63 mm (with no scattering material in place) within a 1-min acquisition time. In contrast, the camera has a detection limit for deep-seated tumours to depths up to 20 mm beneath the skin surface with the SCD of 63 mm and 5 min imaging time. These limitations can be improved by prolonging the image acquisition time and shortening SCD to increase system sensitivity and spatial resolution, but the decrease in the field of view and longer

Figure 6. (a) Gamma, (b) optical and (c) hybrid images of the ^{125}I seeds placed with a separation distance of 3 mm, taken by HGC (1 mm diameter pinhole collimator).

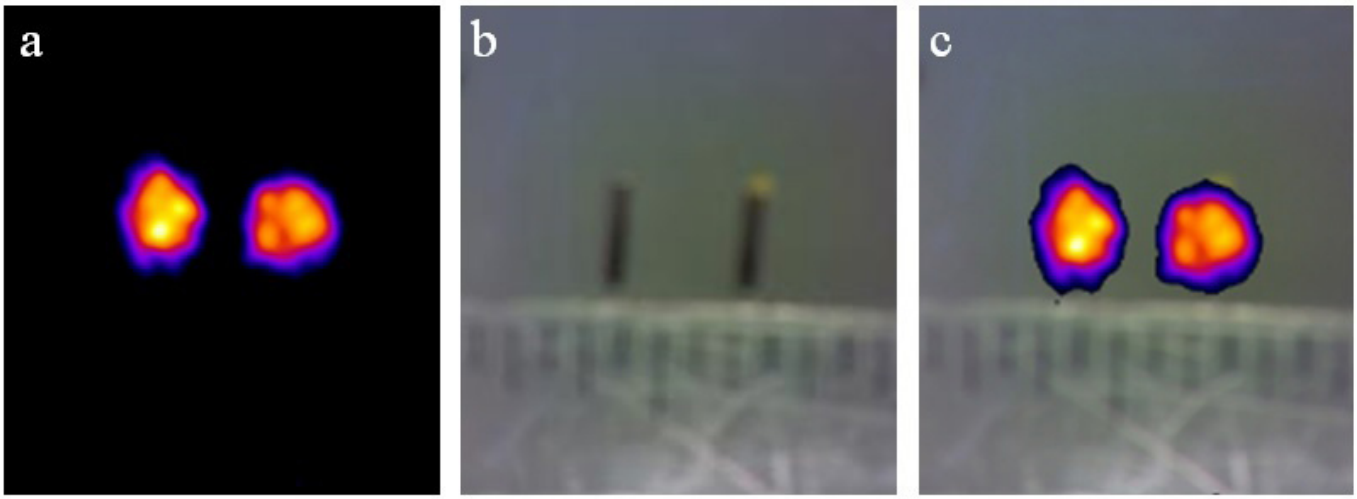

surgery times may pose a challenge. Due to limitations of the availability of ^{125}I seeds for the experimental studies, 2.43 MBq was lower than the activity that is normally used clinically (3–13 MBq), therefore the detectability of deeper tumours (at depths greater than 2 cm) would be expected to be greater than we have measured.

The detectability of ^{125}I seeds may also be enhanced by using larger pinhole collimator (*i.e.* 1 mm in diameter). The camera fitted with 0.5 mm pinhole collimator exhibits lower sensitivity but higher spatial resolution. It could resolve two seeds placed at a separation of 2 mm apart with the SCD of 30 mm and 10 min acquisition time. With the increase of the pinhole diameter (1 mm), the camera was able to resolve seeds at a separation distance of 3 mm. These images could be useful for localising multiple seeds in the same breast which are embedded under mammographic guidance in the case of larger lesions (tumour bracketing) or multiple lesions, in order to aid determination of surgical dissection margins.

Figure 7. Line profiles (five pixel width) drawn across the centre of the hot spot(s) in the gamma images (right side) with seeds placed (a) 1 mm and (b) 2 mm apart, acquired using HGC mounted with 0.5 mm pinhole collimator. The connecting lines were the profiles fitted with Gaussian function.

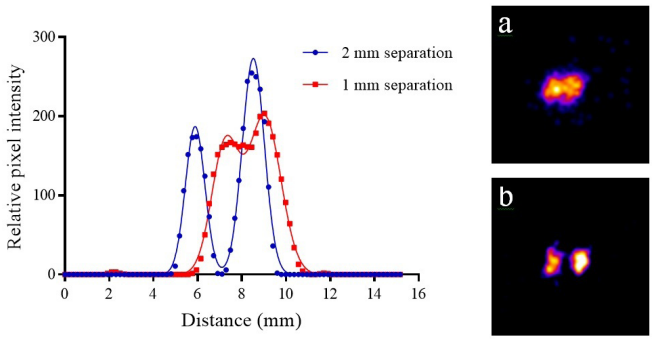

In addition to the application of RSL in breast conserving surgery, it is apparent that SFOV HGC may offer potential clinical value with the use of ^{125}I radioactive seeds for brachytherapy. This technique is used to treat a range of tumours including prostate, oesophageal, head and neck and lung cancers.[19–21] In certain instances, problems have been encountered when seed loss or migration has occurred.[22,23] Due to the high resolution and

Figure 8. (a–c) Gamma images of the dual radionuclide sources acquired using HGC with different acquisition times. (d) Scintigraphic image acquired using a LFOV gamma camera with 2 min acquisition time, phantom placed at SCD of 2 cm and matrix size of 128 × 128. (e) Fused SPECT and CT images (coronal slice) obtained using SPECT-CT with matrix size of 128 × 128, 120 projections over a 180° rotation in which 20 s per projection for each detector. Two separate SPECT images of ^{125}I and ^{99m}Tc were generated simultaneously in addition to the CT image (3 sets of image data) during the imaging session. Minor green spot was found at the ^{125}I seed holder due to contamination of ^{99m}Tc to the phantom.

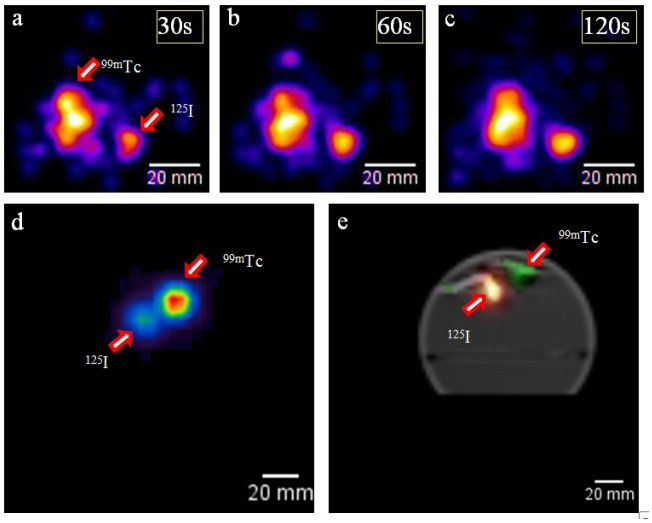

Figure 9. (a) Photograph of the clinical imaging assessment setup. (b) Post-processed hybrid image illustrated a bright blob at the position of "C".

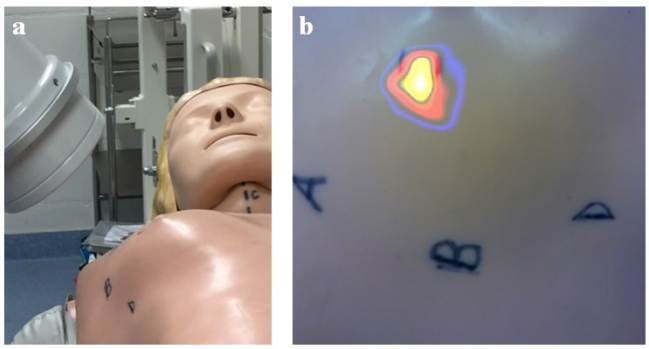

compact design of the HGC and the production of hybrid optical-gamma images this may provide added values in detecting and locating seeds which have been lost or migrated to other regions of the body such as to the chest, abdomen and pelvis.

CONCLUSION

These studies demonstrate the first results of the feasibility and capability of a SFOV hybrid gamma camera in the detection and imaging of ^{125}I radioactive seeds indicating the potential use in RSL guiding the intraoperative surgical procedure, with the added benefit of providing hybrid optical-gamma images for medico-legal records. The camera has sufficient sensitivity to detect the lower energy gamma rays (~35.5 keV) emitted from ^{125}I and the spatial resolution was high enough to resolve a radioactive seed of small physical size (~1 mm in diameter). Further improvements of the camera's ability to detect multiple radionuclides simultaneously could expand the application of the imaging system in other perioperative imaging procedures in future.

ACKNOWLEDGMENTS

The authors would like to thank to the Science and Technologies Facilities Council (UK) for the research funding, GE Healthcare Life Sciences (UK & US) for supplying the I-125 seeds, Simon Lawes for operating the SPECT-CT camera, Clare Jacobs for her technical advice on gamma probe and all volunteers who participated in the clinical simulation studies. The authors would also like to thank the Director General of Health Malaysia for his permission to publish this article.

CONFLICTS OF INTEREST

This project was funded by the Science and Technologies Facilities Council (UK). The authors declare that there is no conflict of interest.

REFERENCES

1. Cancer Research UK. Breast cancer statistics [Internet]. 2018. Available from: http://www.cancerresearchuk.org/health-professional/cancer-statistics/statistics-by-cancer-type/breast-cancer [2018 Sept 3].
2. Cady B, Stone MD, Schuler JG, Thakur R, Wanner MA, Lavin PT. The new era in breast cancer. invasion, size, and nodal involvement dramatically decreasing as a result of mammographic screening. *Arch Surg* 1996; **131**: 301–8.
3. Lovrics PJ, Cornacchi SD, Vora R, Goldsmith CH, Kahnamoui K. Systematic review of radioguided surgery for non-palpable breast cancer. *Eur J Surg Oncol* 2011; **37**: 388–97. doi: https://doi.org/10.1016/j.ejso.2011.01.018
4. Pouw B, de Wit-van der Veen LJ, Stokkel MPM, Loo CE, Vrancken Peeters M-JTFD, Valdés Olmos RA. Heading toward Radioactive seed localization in non-palpable breast cancer surgery? A meta-analysis. *J Surg Oncol* 2015; **111**: 185–91. doi: https://doi.org/10.1002/jso.23785
5. Milligan R, Pieri A, Critchley A, Peace R, Lennard T, O'Donoghue JM, et al. Radioactive seed localization compared with wire-guided localization of non-palpable breast carcinoma in breast conservation surgery- the first experience in the United Kingdom. *Br J Radiol* 2018; **91**: 20170268. doi: https://doi.org/10.1259/bjr.20170268
6. Gray RJ, Salud C, Nguyen K, Dauway E, Friedland J, Berman C, et al. Randomized prospective evaluation of a novel technique for biopsy or lumpectomy of nonpalpable breast lesions: Radioactive seed versus wire localization. *Ann Surg Oncol* 2001; **8**: 711–5. doi: https://doi.org/10.1007/s10434-001-0711-3
7. Goudreau SH, Joseph JP, Seiler SJ. Preoperative Radioactive seed localization for nonpalpable breast lesions: technique, pitfalls, and solutions. *Radiographics* 2015; **35**: 1319–34. doi: https://doi.org/10.1148/rg.2015140293
8. Pouw B, der Veen LJdeW-van, Hellingman D, Brouwer OR, Peeters M-JTV, Stokkel MP, et al. Feasibility of preoperative $^{(125)}$I seed-guided tumoural tracer injection using freehand SPECT for sentinel lymph node mapping in non-palpable breast cancer. *EJNMMI Res* 2014; **4**: 19. doi: https://doi.org/10.1186/s13550-014-0019-5
9. Pouw B, de Wit-van der Veen LJ, van Duijnhoven F, Rutgers EJT, Stokkel MPM, Valdés Olmos RA, et al. Intraoperative 3D navigation for single or multiple ^{125}I-Seed localization in breast-preserving cancer surgery. *Clin Nucl Med* 2016; **41**: e216–20. doi: https://doi.org/10.1097/RLU.0000000000001081
10. Lees JE, Bugby SL, Bhatia BS, Jambi LK, Alqahtani MS, McKnight WR, et al. A small field of view camera for hybrid gamma and optical imaging. *J. Inst.* 2014; **9**: C12020. doi: https://doi.org/10.1088/1748-0221/9/12/C12020
11. Lees JE, Bugby SL, Alqahtani MS, Jambi LK, Dawood NS, McKnight WR, et al. A multimodality hybrid Gamma-Optical camera for intraoperative imaging. *Sensors* 2017; **17**: 55409 Mar 2017. doi: https://doi.org/10.3390/s17030554
12. Bugby SL, Lees JE, Bhatia BS, Perkins AC. Characterisation of a high resolution small field of view portable gamma camera. *Phys Med* 2014; **30**: 331–9. doi: https://doi.org/10.1016/j.ejmp.2013.10.004
13. Perkins AC, Britten AJ. Specification and performance of intra-operative gamma probes for sentinel node detection. *Nucl Med Commun* 1999; **20**: 309–14. doi: https://doi.org/10.1097/00006231-199904000-00005
14. Ng AH, Clay D, Blackshaw PE, Bugby SL, Morgan PS, Lees JE, et al. Assessment of the performance of small field of view gamma

cameras for sentinel node imaging. *Nucl Med Commun* 2015; **36**: 1134–42. doi: https://doi.org/10.1097/MNM.0000000000000377

15. Cherry SR, Sorenson JA, Phelps ME. Physics in Nuclear Medicine. In: *3rd Ed*. Philadelphia PA: Elsevier; 2003.
16. Pouw B, van der Ploeg IMC, Muller SH, Valdés Olmos RA, Janssen-Pinkse LK, Oldenburg HSA, et al. Simultaneous use of an (125)I-seed to guide tumour excision and (99m)Tc-nanocolloid for sentinel node biopsy in non-palpable breast-conserving surgery. *Eur J Surg Oncol* 2015; **41**: 71–8. doi: https://doi.org/10.1016/j.ejso.2014.10.046
17. Mediso Medical Imaging System. Nucline™ TH [Internet]. 2016. Available from: http://www.mediso.com/ [2018 Apr 19].
18. Garner HW, Bestic JM, Peterson JJ, Attia S, Wessell DE. Preoperative Radioactive seed localization of nonpalpable soft tissue masses: an established localization technique with a new application. *Skeletal Radiol* 2017; **46**: 209–16. doi: https://doi.org/10.1007/s00256-016-2529-x
19. Zhang W, Li J, Li R, Zhang Y, Han M, Ma W. Efficacy and safety of iodine-125 radioactive seeds brachytherapy for advanced non-small cell lung cancer-a meta-analysis. *Brachytherapy* 2018; **17**: 439–48. doi: https://doi.org/10.1016/j.brachy.2017.11.015
20. Lei G-Y. Safety and efficacy of CT-guided percutaneous and transtracheal iodine-125 radioactive seeds implantation for recurrence and metastasis of esophageal carcinoma in the upper posterior mediastinum. *Brachytherapy* 2018; **17**: S60–S61. doi: https://doi.org/10.1016/j.brachy.2018.04.097
21. Stannard C, Maree G, Tovey S, Hunter A, Wetter J. Iodine-125 brachytherapy in the management of squamous cell carcinoma of the oral cavity and oropharynx. *Brachytherapy* 2014; **13**: 405–12. doi: https://doi.org/10.1016/j.brachy.2014.02.443
22. Sugawara A, Nakashima J, Kunieda E, Nagata H, Mizuno R, Seki S, et al. Incidence of seed migration to the chest, abdomen, and pelvis after transperineal interstitial prostate brachytherapy with loose (125)I seeds. *Radiat Oncol* 2011; **6**: 130. doi: https://doi.org/10.1186/1748-717X-6-130
23. Maletzki P, Schwab C, Markart P, Engeler D, Schiefer J, Plasswilm L, et al. Late seed migration after prostate brachytherapy with Iod-125 permanent implants. *Prostate Int* 2018; **6**: 66–70. doi: https://doi.org/10.1016/j.prnil.2017.09.003